Advanced Studies in Theoretical Physics
Vol. 9, 2015, no. 6, 263 - 272
HIKARI Ltd, www.m-hikari.com
http://dx.doi.org/10.12988/astp.2015.512

Fast Fourier Computational Analysis of the Optical Properties of Lead Sulphide Thin Film

Moses Eterigho Emetere [1*] and Uno Essang Uno[2]

[1]Department of Physics, Covenant University, Ota, Nigeria
[2]Department of Physics, Federal University of Technology, Minna, Nigeria
[*] Corresponding author

Abstract

The physics of the absorbance of lead sulphide (PbS) is still unknown. The multiplication of experimental research all points to fact that the quantum confinement of PbS is dependent on the growing technique and dopant inherent properties. Hence, the evidence of quantum confinement impairment may not be visible but it contributes to the inefficiency of the PbS. A theoretical probe was done using the Fourier computational analysis of series of governing equations-derived from text. The actualization of the quantum confinement impairment was successful- showing that the extreme size increase or decrease may not be advantageous for industrial use.

Keywords: lead sulphide thin film, optical properties, quantum confinement, impairement, chalcogenide, Fourier computational analysis

Introduction

In the 1930s, the lead sulphide was discovered. It works on material as infrared detector and has wide range of military application. In recent times, it is used as light emitting diodes, gas spectrometer, fabricating thin film integrated circuits and computer memories, wave guides switches modulators or laser detectors in integrated optics for measuring gas chemical specie in the laboratory and the lower atmosphere. Lead sulphide (PbS) is a semiconducting chalcogenide with direct bandgap of 0·41 eV and thus serves as a good transducer in many optical-electrical devices e.g. photovoltaic modules. The wide range of lead sulphide is pro-

portional to its industrial or laboratory preparation techniques. The industrial or laboratory preparation techniques include chemical bath deposition (CBD) method, spray pyrolysis, chemical vapour deposition (CVD) and magnetic sputtering (Bhatt et al., 2012; Uno et al.,2014a,b; Emetere et al., 2013; Devi et al, 2007; Obaid et al.,2012). Preparation technique has engendered the quantum size effect (Mahdi et al., 2012), positional doping effect (Uno et al., 2014) e.t.c. which is of interest to physicist. For example, the lead sulphide semiconductor nano-crystals showed an improved electronic band structure and gap when the quantum confinement is worked upon (Kang et al., 1997). Quantum confinement occurs in a semiconductor crystallite when its excitons are squeezed via its diameter reduction i.e. lower than the size of its exciton Bohr radius. Generally, there are weak and strong confinement regimes. Hence, the electronic and optical properties are highly tunable at this regime. During this state, continuous energy state may keep the band gap at its original energy except there is a change in size. Figure 1 expresses the expected quantum confinement in nano structure and bulk materials. PbS exhibit strong quantum size effects below excitonic Bohr radius (Tang et al., 2010). Its energy band gap (of its nanocrystals) can be tuned to anywhere between 0.41 (bulk) to 4 eV. The bandgap width of lead sulphide (PbS) is very sensitive to finite-size effects. Hence, it manifests high increase of optical absorption energy via its particulate size i.e. quantum dot or bulk PbS. Its optical bandgap in the PbS quantum dot increases up to 5.2 eV compared to the 'bulk' PbS value which is given as ~0.4 eV at room temperature (Hoffmann et al., 2000). In this paper, we propose via the Fourier computational analysis- the quantum confinement impairment initiated by the structure and interplane of the PbS.

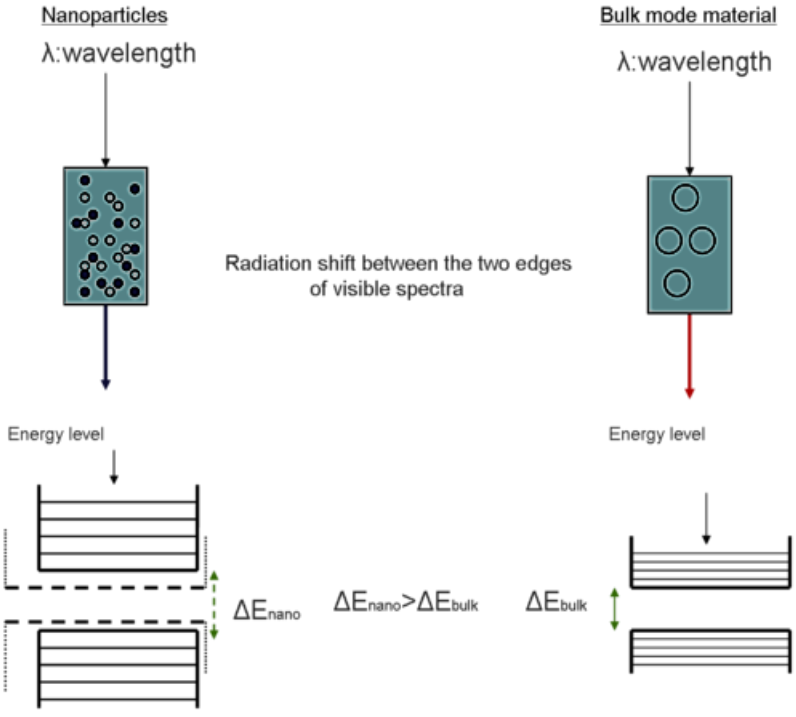

Figure 1: Quantum confinement effects on the energy difference between energy states and band gap (Retrieved from wikipedia)

Theoretical background

The Debye-Scherer equation is used to determine the particle sizes of the samples. It is written as

$$\boldsymbol{D = \frac{0.9\lambda}{Bcos\theta}} \quad (1)$$

Here, D (nm) is the average particle size, λ (nm) is the X-ray wavelength, θ (degrees) is the diffraction angle, and B (nm) is the maximum peak width in half-height. The particle size determines the quantum yield (Emetere, 2013). Therefore the fluorescence quantum yield may be written as

$$\boldsymbol{\phi_f = \frac{N_e(\lambda)}{N_a(\lambda)}} \quad (2)$$

Here, $\boldsymbol{N_e(\lambda)}$ is the number of the emitted photons, $\boldsymbol{N_a(\lambda)}$is the number of the absorbed photon, and $\boldsymbol{\phi_f}$ is the fluorescence quantum yield. Experimentally, it is not easy to determine the absolute quantum yield because this method requires sophisticated instrumentation. However, few theoretical formulas had been propounded. The validity of such theories is still unclear because it did not adequately estimate the number of the emitted photons. Hence, part of the objective of this paper is to propound a new technique for estimating the quantum yield. From the theory of lasers (Emetere, 2014), $\boldsymbol{J(\theta)}$ which is emitted photon factor represents the optical transport of the combined multilayered material. It is represented as

$$\boldsymbol{J(\theta) = \int_{\theta_1}^{\theta_2} \epsilon_\lambda{}^{\iota}(\theta) cos\theta sin\theta d\theta} \quad (3)$$

Here, $\epsilon_\lambda{}^{\iota}$ is the spectral directional emissivity. Using equation [1], equation [3] becomes

$$\boldsymbol{J(\theta) = \frac{0.9\lambda}{BD}\int_{\theta_1}^{\theta_2} \epsilon_\lambda{}^{\iota}(\theta) sin\theta d\theta} \quad (4)$$

Wilkins et al., (2010) investigated the X-ray spectral directional emissivity of the accretion disc in this Narrow Line Seyfert 1 galaxy 1H0707-495 which gave a value of 1.1255.

$$J(\theta) = \frac{1.01295\lambda}{BD}\cos(\theta) \quad (5)$$

Where $\cos(\theta) = \cos(\theta_2) - \cos(\theta_1)$. Let the first excited state calculated by Emetere (2013, 2014) be equal to the estimated number of absorbed photon i.e. $N_a(\lambda) = 2 - m \,.\, \omega_1 M_y \mathrm{T}_1$

Here, $M_y = \mathrm{A}\sin(\omega t)$, $m \,.\, \omega_1 M_y \mathrm{T}_1 \gg 2$. Therefore, $N_a(\lambda) = -m \,.\, \omega_1 \mathrm{A}\sin(\omega t)\mathrm{T}_1$

Where $\alpha = \omega_1 \mathrm{A}\sin(\omega t)$ and $N_a(\lambda) \approx \alpha$

Here α is the absorbance. Then, on the condition that $\omega t = \theta$

$$\phi_f = \frac{1.01295\lambda}{\omega_1 ABD}\cot(\theta) \tag{6}$$

Virtual Experiment: The Fourier Computation Analysis of the Lead Sulphide

The virtual experiment was done using the MATLAB. First, we assumed the bulk, thin film and nanostructure PbS via the particle sizes of the samples. The experimentation is shown in figures 1a-h,

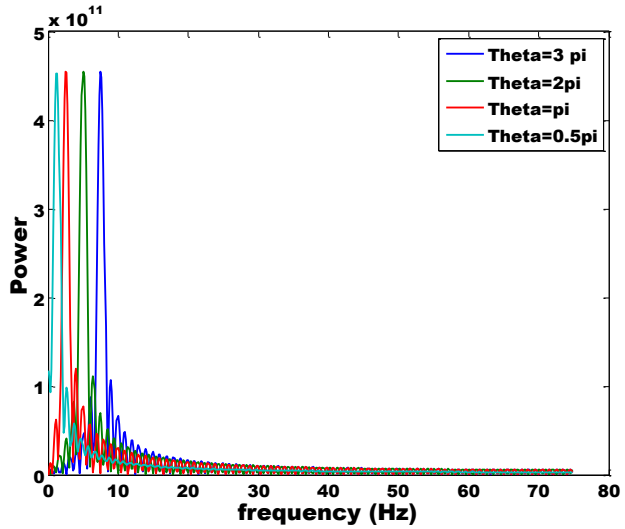

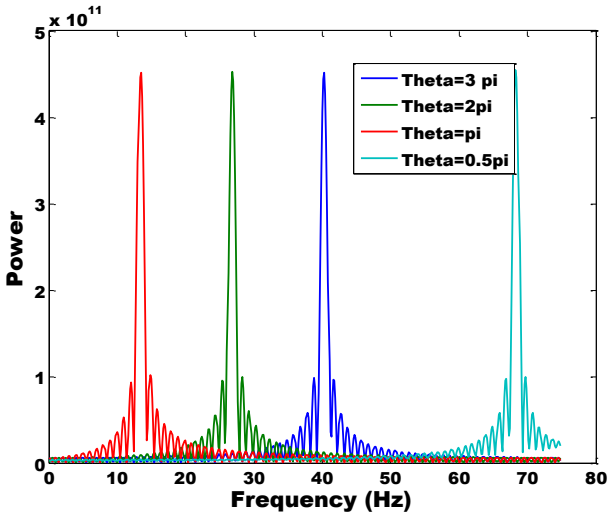

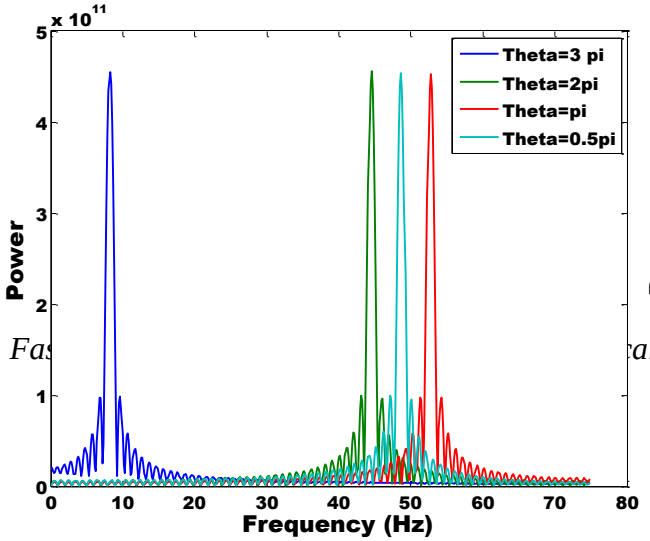

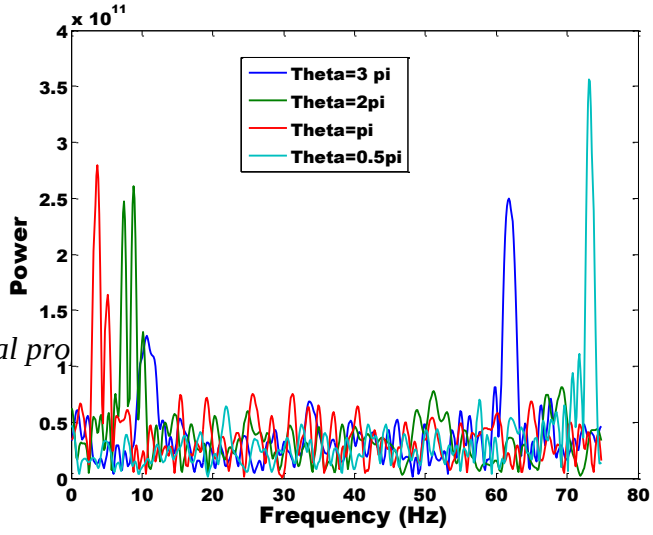

Fas *al pro*

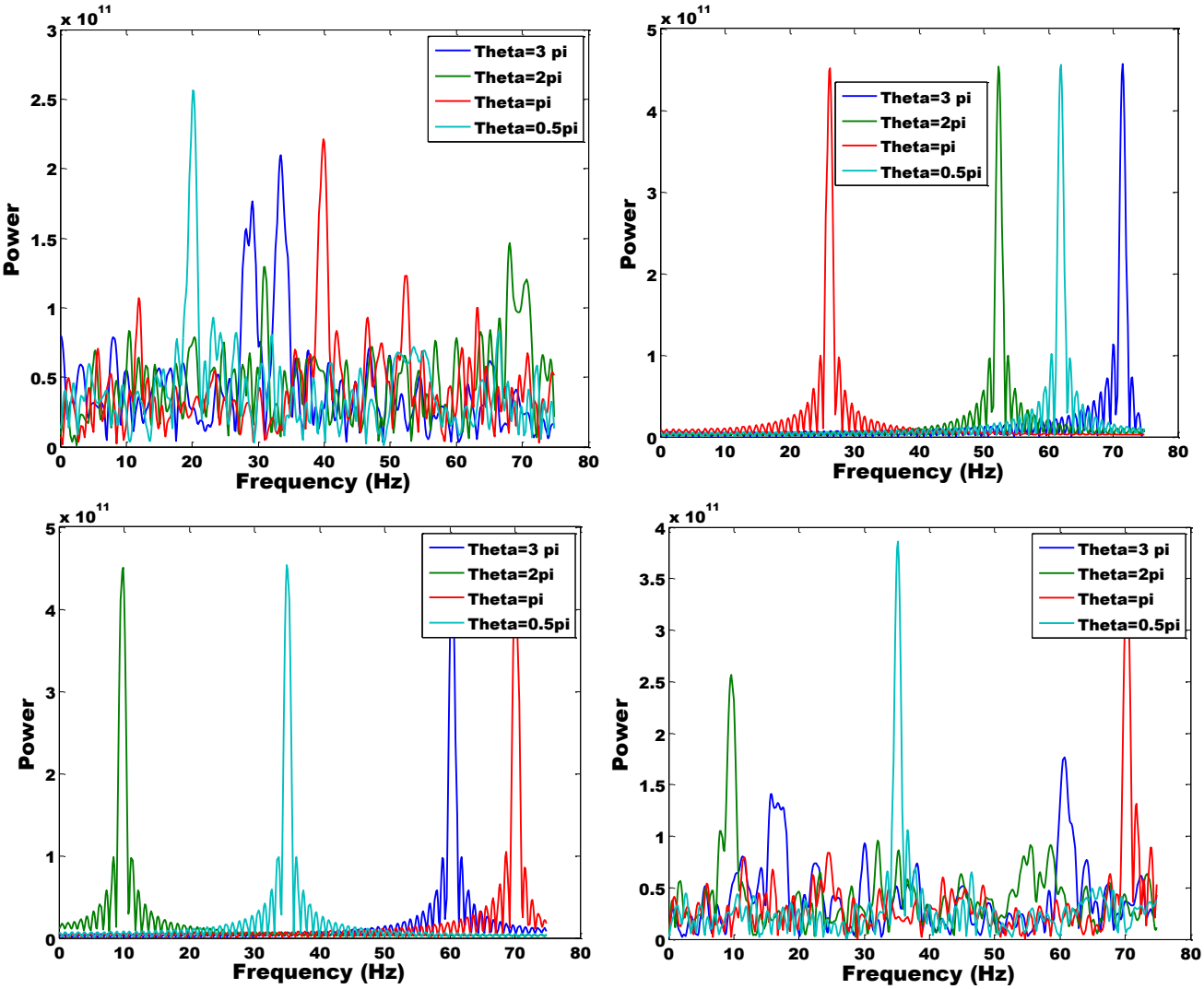

Figure 1a-h: mimicked Fourier analysis of XRD pattern. An evidence of quantum confinement shift with respect to PbS size.

The experimentation mimics the intensity-theta graph of the X-ray diffraction (XRD). The XRD pattern was generated via equation (5). Two cases were considered to elaborate on the diffraction angle. First, the normal diffraction angle which shows the basic four diffraction peaks of the PbS i.e. (200), (220), (111) and (222). These normal diffraction were obtained at Theta= $\pi/2$, π, 2π and 3π. Here we propose that the (111) diffraction peak is on 2π (green color), while the (200) is on $\pi/2$ (sky blue color) because of its consistency in the simulations. Under

strict assumptions, when the counting time (t) tends to unity i.e. $\boldsymbol{t \rightarrow 1}$, $\boldsymbol{\omega t = \theta \approx f}$. Hence, the horizontal axis of the Figure 1a-h can be referred to diffraction angle. The vertical axis of Figure 1a-h via proportionality can be equated to relative intensity. Therefore, the simulations of Figure 1a-h can be considered a theoretical XRD. Figure 1a is possible at normal diffraction angle i.e. if the compound is homogenous. However, the focus of this study is the PbS which is a heterogeneous compound. Hence the diffraction angle in practical sense follows an exponential trend (see Figure 2). Therefore Figures 1b-h are results obtained from an experimentally valid exponential trend of the diffraction angle. Figures 1b,c,f,g are theoretical validation of changing quantum confinement due to Bauschinger effect.

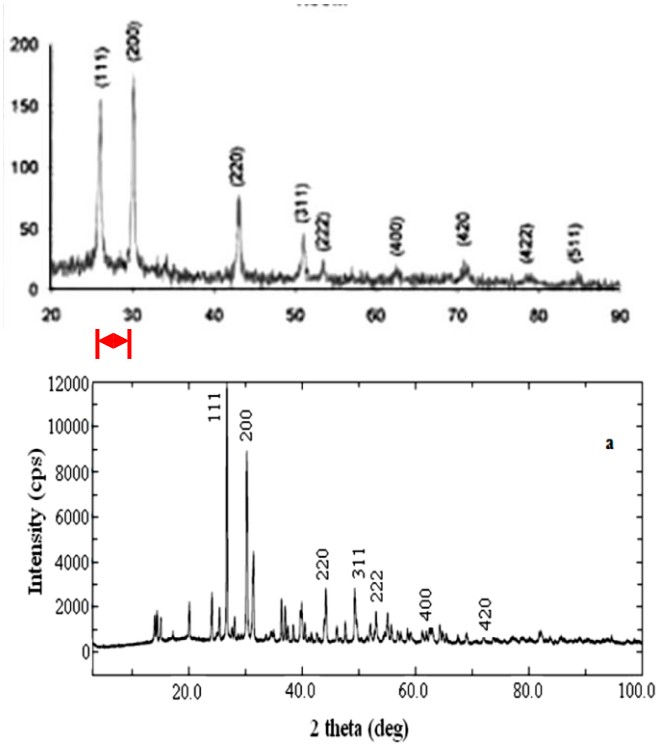

Figure 2a-b: Experimental XRD showing varying interval between (111) and (200). Diagrams are obtained from Choudhury et al.,(2009) and Borhade et al., (2012).

Evidence of quantum confinement impairment can be seen in Figure 1d though not clear. However, the evidence of quantum confinement impairment is clearer in Figure 1e & h (see the red arrows over the diffraction peak-blue line). While Figure 1e shows that the first-kind quantum confinement impairment is between 27^{o}and 32^{o}. This kind is common with doped nanostructure XRD- see the experimental evidence shown in Figure 3.

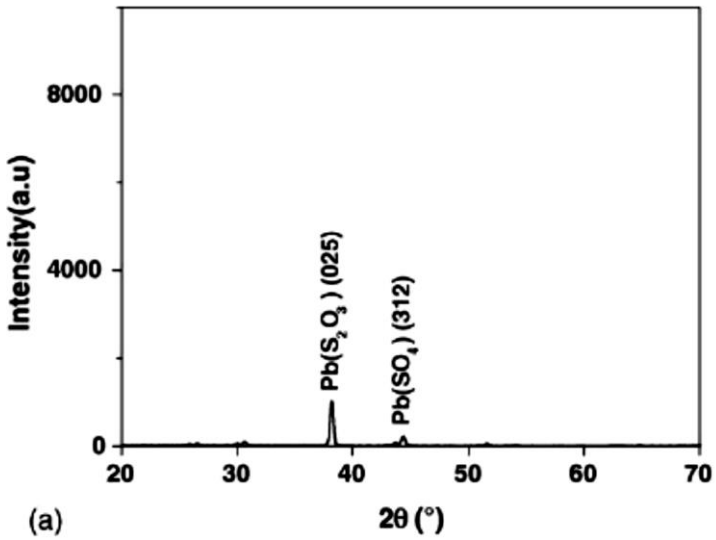

Figure 3: Evidence of first – kind quantum confinement impairment for doped nanostructure PbS (Seghaier et al., 2006)

The second kind of quantum confinement impairment can be seen in figure 1h between 18^{o}and 62^{o}. Though an experimental example was cited for this kind of quantum confinement impairment. Hence, the authors proposed this kind of occurrence in a super nanostructure PbS. This shows that the crystallography of the PbS is quite unique. In other words, PbS is potentially viable for predictive study and applications.

Conclusion

The PbS do not only decrease the density of localized states or improves the crystallinity of the films. Its impact on the quantum confinement of the sample as

shown in both theoretical and experimental XRD. However, the initiated Bauschinger effect-amongst other effects are responsible for thermal gradient truncation in some heterogeneous compounds. Quantum confinement impairment enables a sample to mimic several states. This may be advantageous for PbS industrial applications. Particulate size of a heterogeneous compound is directly proportional to the formations of various quantum confinements. When the results are compared with past research on PbS, the quantum confinement impairment are more evident. Hence, the preparation or growing technique of PbS defines the dimension of the quantum confinement impairment.

Acknowledgements. The author acknowledges their host institutions. This paper has no conflicting interest.

Reference

[1] Borhade, A.V., and B.K.Uphade, A Comparative Study on Characterization and Photocatalytic activities of PbS and Co doped PbS Nanoparticles, *Chalcogenide Letters*, 9(7), (2012), 299 – 306.

[2] Choudhury, N. and B K Sarma, Structural characterization of lead sulfide thin films by means of X-ray line profile analysis, *Bull. Mater. Sci*., 32 (1), (2009), 43–47. http://dx.doi.org/10.1007/s12034-009-0007-y

[3] Devi R, Purkayastha P, Kalita P K and Sarma B K. Synthesis of nanocrystalline CdS thin films in PVA matrix *Bull. Mater. Sci*. 30 (2007), 123. http://dx.doi.org/10.1007/s12034-007-0022-9

[4] Emetere, Moses E., Modeling the Non-Single Exponential photoluminescence Decay Using the Boubaker Polynomial Expansion Scheme. *Journal of Advance Physics*, 2 (3), (2013), 213-215. http://dx.doi.org/10.1166/jap.2013.1062

[5] Emetere, Moses E., Profiling Laser Induced Temperature Fields for Superconducting Materials Using Mathematical Experimentation. *Journal of Thermophysics and Heat Transfer* 28(4), (2014), 700-707. http://dx.doi.org/10.2514/1.t4407

[6] Emetere, Moses E., and B. Nikouravan. Femtosecond Spin Dynamics Mechanism Probed By the Bloch NMR -Schrödinger Mainframe. International Journal of Fundamental Physical Sciences 4(4), (2014) 105-110. http://dx.doi.org/10.14331/ijfps.2014.330073

[7] Emetere, Moses E., Mathematical Modeling of Bloch NMR to Solve a Three Dimensional- Schrodinger Time Dependent Equation. *Applied Mathematical Sciences,* 8 (56), (2014), 2753 – 2762.

[8] Emetere, Moses E., Mathematical Modeling of Bloch NMR to Solve the Schrodinger Time Dependent Equation. *The African Review of Physics,* 8(10), (2013), 65-68.

[9] Ho SM, Anuar K. Tan, WT. Thickness Dependent characteristics of chemically deposited tin sulphide films. *Universal Journal of Chemistry*. 1(4), (2013), 170-174.

[10] Hassan Karami, Mina Ghasemi, Sara Matini. Synthesis, Characterization and Application of Lead Sulfide Nanostructures as Ammonia Gas Sensing Agent, *Int. J. Electrochem. Sci.,* 8 (2013), 11661 – 11679.

[11] Hoffmann, E., P. Entel. Structure and Dynamics of Heterogeneous Systems. *From Solids to Clusters*, 54(2000), 148–155. http://dx.doi.org/10.1142/9789812793652_0014

[12] Kang, I., Wise, F.W. Electronic structure and optical properties of PbS and PbSe quantum dots. *J. Opt. Soc. Am. B-Opt. Phys*. 14 (1997), 1632-1646. http://dx.doi.org/10.1364/josab.14.001632

[13] Mahdi,M.A., J.J. Hassan, S.S. Ng, Z. Hassan. Growth of CdS nanosheets and nanowires through the solvothermal method, *J. Cryst. Growth*, 359(2012), 43-48. http://dx.doi.org/10.1016/j.jcrysgro.2012.08.017

[14] Obaid,A.S., M.A Mahdi, Z Hassan, M Bououdina, Characterization of nanocrystalline PbS thin films prepared using microwave-assisted chemical bath deposition, Materials Science in Semiconductor Processing 15(2012), 564–571. http://dx.doi.org/10.1016/j.mssp.2012.04.009

[15] Prakash V, Jumate N, Popescu G, Moldovan M, Prejmeriean C. Studies of some electrical and photoelectrical properties of PbS films obtained by sonochemical methods. *Chalcogenide Lett.* 7(2004), 95-100.

[16] Sandip V. Bhatt, M.P. Deshpande, Bindiya H. Soni, Nitya Garg, Sunil H. Chaki. Chemical Bath Deposition of Lead Sulphide (PbS) Thin Film and their Characterization.*Solid State Phenomena*, 209(2013), 111-115.

http://dx.doi.org/10.4028/www.scientific.net/ssp.209.111

[17] Seghaier,S., N. Kamouna, R. Brini, A.B. Amarac, Structural and optical properties of PbS thin films deposited by chemical bath deposition, Materials Chemistry and Physics 97 (2006), 71–80.
http://dx.doi.org/10.1016/j.matchemphys.2005.07.061

[18] Tang,J., X. Wang, L. Brzozowski, D. Aaron, R. Barkhouse, R. Debnath, L. Levina, E.H. Sargent. Schottky Quantum Dot Solar Cells Stable in Air under Solar Illumination, *Adv. Mater*. 22 (2010), 1398.
http://dx.doi.org/10.1002/adma.200903240

[19] Uno E. Uno, Moses E. Emetere, Mathew Aplha. Crystalline Grain Size Effects on the Conductivity of the Doped Tin Dioxide (SnO_2) With Zinc (Zn). *Journal of Ovonic Research*, 10 (3), (2014), 83-88.

[20] Uno E. Uno, Moses E. Emetere, Akhpelor A. Ohiozebau, Enebeli C. Benaiah, Onogu A. Williams. Evidence of Positional Doping Effects on the Optical Properties of Doped Tin Dioxide (SnO_2) With Zinc (Zn). *Journal of Ovonic Research* 10 (4), (2014) 141-147.

[21] Wilkins, D. R., and A. C. Fabian, Determination of the X-ray reflection emissivity profile of 1H0707-495, Mon. Not. R. Astron. Soc. 000, (2010) 1–9.

Received: January 17, 2015; Published: March 9, 2015